

# Exact-diagonalization method for soft-core bosons in optical lattices using hierarchical wavefunctions

Deepak Gaur,<sup>1,2</sup> Hrushikesh Sable,<sup>1,3</sup> and D. Angom<sup>4</sup>

<sup>1</sup>Physical Research Laboratory, Ahmedabad - 380009, Gujarat, India

<sup>2</sup>Indian Institute of Technology Gandhinagar, Palaj, Gandhinagar - 382355, Gujarat, India

<sup>3</sup>Department of Physics, Virginia Tech, Blacksburg, Virginia 24061, USA

<sup>4</sup>Department of Physics, Manipur University, Canchipur - 795003, Manipur, India

In this work, we describe a new technique for numerical exact-diagonalization. The method is particularly suitable for cold bosonic atoms in optical lattices, in which multiple atoms can occupy a lattice site. We describe the use of the method for Bose-Hubbard model as an example, however, the method is general and can be applied to other lattice models. The proposed numerical technique focuses in detail on how to construct the basis states as a hierarchy of wavefunctions. Starting from single-site Fock states we construct the basis set in terms of row-states and cluster-states. This simplifies the application of constraints and calculation of the Hamiltonian matrix. Each step of the method can be parallelized to accelerate the computation. In addition, we have illustrated the computation of the spatial bipartite entanglement entropy in the correlated  $\nu = 1/2$  fractional quantum Hall state.

## I. INTRODUCTION

Only a few problems in quantum many-body systems are analytically solvable. Often, one resorts to numerical techniques to gain some insights into these systems. Numerical mean-field methods are relatively straightforward and easy to use [1], however, it fails to capture the correlations and entanglement of the underlying quantum system. Beyond the mean-field theory, Quantum Monte Carlo (QMC) based methods like the stochastic series expansion [2, 3] are powerful numerical techniques. QMC is often used to study the reliable approximate properties of the system in thermodynamic limit. However, for fermionic systems like frustrated quantum spins QMC suffers from the “sign problems” [4]. In addition, a direct access to the full quantum state is not possible with QMC. To obtain the complete information of the system, the numerical exact-diagonalization (ED) is useful. As the name suggests, the Hamiltonian matrix is “exactly” diagonalized after constructing the basis states, and setting up the Hamiltonian matrix in these basis states. This gives the eigenstates and the energy spectrum of the system. For most of the studies on quantum-mechanical systems at low temperatures, the low energy spectrum namely, the ground state and few excited states can describe the properties of the system. This simplicity allows the usage of well-known Lanczos algorithm for faster numerical diagonalization [5, 6]. The ED method offers the advantage of access to the exact solution, but simultaneously requires a lot of computational resources which grows with complexity of the problem. For instance, for the system of spins on a lattice, the Hilbert space of the system grows exponentially with the lattice size. Thus, ED limits the system size that one can study. In the literature, there exists large-scale ED studies for spin  $1/2$  kagome Heisenberg antiferromagnet with  $\approx 40 - 50$  spins [7, 8], bosonic fractional quantum Hall on a  $12 \times 4$  lattice [9]. Some excellent reviews on ED technique are [10–12].

In this work, we shall describe the ED technique in the context of cold bosons in optical lattice where the restricted itinerancy of atoms simplifies the Hamiltonian matrix diagonal-

ization. These quantum systems serve as excellent quantum simulators to study various condensed matter systems [13], as they allow a good control and easy tunability over the system parameters in the experiments [14, 15]. The Bose-Hubbard model (BHM) is a prototypical model that captures the low-energy physics of these bosonic atoms [16–18]. Certain mean-field methods like Gutzwiller [19–21] provide some qualitative insights, however, do not capture the correlations accurately. There are some studies and reviews on ED method for BHM [22, 23]. One such area where ED has been immensely used is in the topological phases like the quantum hall states that can be realized with the cold atoms in the experiments with the help of synthetic gauge fields [24–26]. Mean-field methods are not suitable for studying these strongly correlated phases. Various proposals on the realization of bosonic analogues of fractional quantum Hall (FQH) states with these systems are covered in some excellent reviews [27–30]. Recently,  $\nu = 1/2$  bosonic fractional quantum Hall (FQH) state have been experimentally realized with these systems [31]. There is immense interest in studying these symmetry protected robust phases and their entanglement characteristics. The bipartite entanglement entropy, obtained by partitioning the system into two distinct subsystems, provides a good measure of correlations in the quantum state [32, 33]. The partitioning can be done in real-space, momentum-space or particle-space. Apart from the entanglement entropy, the study of entanglement spectrum reveals interesting properties of the FQH states. The entanglement spectrum, initially studied by Li and Haldane in the context of FQH effect [34], is now been applied in a variety of fields like topological insulators [35–37], many-body localization [38–40]. It is to be noted that in most of these studies on topological properties, one need to know the eigenfunctions and eigen spectrum of the underlying Hamiltonian, in which case, ED is useful.

In this manuscript, we present an algorithm to perform ED numerically using the hierarchical basis states. The idea is to define the basis states as tensor product over appropriate cluster-states and/or rows-states. The row-state is defined as the tensor products over single-site Fock states in the row and represents the configuration of particles along the row. And,

the cluster-states are defined as the tensor product over row-states. This hierarchical construction enables putting restrictions on the occupancies in rows, and the entire state as a whole, thereby optimizing the size of the Hilbert space. The construction of the Hamiltonian matrix is optimized by computing only non-zero matrix elements, thereby reducing the matrix construction time substantially particularly for sparse Hamiltonian matrix. This is achieved by identifying the bra state which contributes to a non-zero matrix element corresponding to the action of any term of the Hamiltonian on a ket state. The bra state is identified among the basis states using a sequence of bisection searches. The constructed matrix can be diagonalized for obtaining the eigen-states and energy spectrum of the system. Afterwards, we discuss the utilization of the construction procedure employed in the basis state generation for the computation of spatial bi-partite entanglement entropy. We have illustrated the algorithm by studying the bi-partite entanglement in the  $\nu = 1/2$  bosonic FQH state on a  $8 \times 8$  lattice. We find that the entanglement entropy follows the ‘‘area law’’, however, the topological entanglement entropy deviates from the theoretical estimates which may be due to the finite size of the lattice.

We have organized the remainder of this article as follows. In Sec. II, we describe our implementation of the ED technique in terms of row-states, as the fundamental building blocks. We describe the construction of the set of basis states, and that of the Hamiltonian in this section. This is followed by Sec. III, where we discuss the modified construction procedures when additional constraints are imposed for filtering out the basis states. These constraints reduce the size of the Hilbert space. In Sec. IV, we demonstrate the usage of the algorithm for studying the spatial bi-partite entanglement in the  $\nu = 1/2$  bosonic FQH state. Finally, we conclude in Sec. V.

## II. COMPLETE BASIS SET

Consider a system of ultracold bosonic atoms loaded in a 2D optical lattice and to simplify the description, consider the geometry to be square. Such a system is well described by the Bose-Hubbard Hamiltonian given

$$\hat{H}_{\text{BHM}} = \sum_{p,q} \left[ -J \left( \hat{b}_{p+1,q}^\dagger \hat{b}_{p,q} + \hat{b}_{p,q+1}^\dagger \hat{b}_{p,q} + \text{H.c.} \right) + \frac{U}{2} \hat{n}_{p,q} (\hat{n}_{p,q} - 1) - \mu \hat{n}_{p,q} \right] \quad (1)$$

where  $p$  ( $q$ ) are the lattice site index along the  $x$  ( $y$ ) directions,  $\hat{b}_{p,q}$  ( $\hat{b}_{p,q}^\dagger$ ) is the annihilation (creation) operator at lattice site  $(p, q)$ ,  $\hat{n}_{p,q}$  is the number operator, and  $U$  is the on-site interaction strength. The eigenstate of a system with a size of  $K \times L$  can be written as the linear combination,

$$|\Psi\rangle = \sum_{\substack{n_{1,1} \\ \dots \\ n_{p,q} \\ \dots \\ n_{K,L}}} C_{n_{1,1}, \dots, n_{p,q}, \dots, n_{K,L}} |n_{1,1}, \dots, n_{p,q}, \dots, n_{K,L}\rangle, \quad (2)$$

where  $n_{p,q}$  is the occupancy at the lattice site  $(p, q)$ , and  $K$  ( $L$ ) is the number of lattice sites along the  $x$  ( $y$ ) directions. To obtain the ground state or any other excited states, the coefficients  $C_{n_{1,1}, \dots, n_{p,q}, \dots, n_{K,L}}$  corresponding to the basis state  $|n_{1,1}, \dots, n_{p,q}, \dots, n_{K,L}\rangle$  must be defined. The basis states are defined in terms of a hierarchy of multiple lattice sites with the starting point being the single-site Fock states.

### A. Construction of the basis states

Let us denote the occupancy of a lattice site  $(p, q)$  by  $n_{p,q}$  and corresponding Fock state can be represented as  $|n_{p,q}\rangle$ . Although,  $n_{p,q}$  can in principle be any non-negative integer, however, let us consider only  $N_B$  possible choices  $n_{p,q} \in \{0, 1, 2, \dots, N_B - 1\}$ . A configuration of occupancies of lattice sites along the  $q$ th row can then be collectively represented by a ‘‘row-state’’ defined as  $|n_{1,q}, n_{2,q}, \dots, n_{p,q}, \dots, n_{K,q}\rangle \equiv \prod_{p=1}^K |n_{p,q}\rangle$ , where,  $1 \leq p \leq K$  is the lattice site index along the row. In general, the label  $q$  corresponding to the row can be omitted as it is common for all the lattice sites along the row. And, a row state can be defined as

$$|n_1, n_2, \dots, n_p, \dots, n_K\rangle = \prod_{p=1}^K |n_p\rangle. \quad (3)$$

The advantage of defining the row-states is that any configuration of particles in the entire lattice can be expressed as a direct product of the row-states. Thus the row-states are the building blocks of the basis states of the entire lattice system.

The occupancies, as mentioned earlier, can be  $0 \leq n_p \leq N_B - 1$ . Then the total number of possible row-state configurations is  $\alpha = (N_B)^K$ . Each row-state configuration is uniquely identified by the quantum number  $m$  and represented as

$$|\phi\rangle_m \equiv \prod_{p=1}^K |n_p\rangle, \quad (4)$$

with  $m \in \{0, 1, 2, \dots, \alpha - 1\}$ . The quantum number  $m$  and number of particles in the row state  $N_m$  are defined as

$$m = \sum_{p=1}^K n_p N_B^{p-1}, \text{ and } N_m = \sum_{p=1}^K n_p. \quad (5)$$

Using the row-states, we construct multi-row states or ‘‘cluster-states’’, which are the occupancy configurations of a cluster consisting of multiple rows. The cluster-states of two rows is represented as  $|\Phi^2\rangle$ . In the present case the lattice dimension of  $|\Phi^2\rangle$  is  $(K \times 2)$ , and each of the cluster-states is a direct-product of the row-states  $|\phi\rangle_m$  defined in Eq. 4 as

$$|\Phi^2\rangle_M = |\phi\rangle_{m_2} \otimes |\phi\rangle_{m_1}. \quad (6)$$

Here, the label  $M$  corresponds to a two-dimensional vector  $\mathbf{M} = (m_1, m_2)$ . It contains information of the row-states

which constitutes the cluster-state. Thus, the total number of possible two-row cluster-states is  $\alpha^2$ , and for a combination of  $m_1$  and  $m_2$ , the corresponding cluster label is  $M = \alpha(m_2) + m_1$ . Similarly, cluster-states of higher number of rows can be constructed from the direct-product of cluster-states with less number of rows and row-states as

$$\begin{aligned} |\Phi^3\rangle_{M'} &= |\Phi^2\rangle_M \otimes |\phi\rangle_m, \\ |\Phi^4\rangle_{M'} &= |\Phi^3\rangle_M \otimes |\phi\rangle_m. \end{aligned} \quad (7)$$

Considering the hierarchy of the cluster-states, different rank cluster-states with  $q$  rows  $|\Phi^q\rangle_M$  is identified by a vector  $\mathbf{M} = (m_1, m_2, \dots, m_q)$  in a  $q$  dimensional space. The row-state quantum numbers are the components of the vector and each axes represents one of the row states. Various  $q$ -row cluster-states are assigned a unique integer index  $M$  corresponding to the vector label  $\mathbf{M}$  and the number of particles in the state  $N_M$  are

$$M = \sum_{j=1}^q \alpha^{j-1} m_j, \text{ and } N_M = \sum_{i=1}^K \sum_{j=1}^q n_{i,j}. \quad (8)$$

Generalizing the definition of multi-row states, basis states of a system with  $L$  rows and  $K$  columns is constructed as a direct product of two appropriately chosen multi-row states. Each of the basis state  $|\Phi^L\rangle_M$  is identified by an  $L$  dimensional vector  $\mathbf{M} = (m_1, m_2, \dots, m_L)$  and an index  $M$ . For example, the basis for a  $K \times 7$  lattice system can be constructed as direct product of multi-row states  $|\Phi^4\rangle_{M_1}$  and  $|\Phi^3\rangle_{M_2}$  as given below

$$|\Phi^7\rangle_M = |\Phi^4\rangle_{M_1} \otimes |\Phi^3\rangle_{M_2}. \quad (9)$$

The basis states are uniquely identified by a vector  $\mathbf{M}$  and are labelled with an integer  $M$  according to relation given in Eq.8. Thus, in general the basis states of  $K \times L$  can be defined as the direct product

$$|\Phi^L\rangle_M = |\Phi^{L_1}\rangle_{M_1} \otimes |\Phi^{L_2}\rangle_{M_2}, \quad (10)$$

where,  $L = L_1 + L_2$ . Below is a schematic representation showing the occupancies over the lattice which constitutes a basis state being identified as a column vector of row-states which is the essence of Eq.9.

$$\begin{pmatrix} n_{1,L} & n_{2,L} & \cdots & n_{p,L} & \cdots & n_{K,L} \\ \vdots & \vdots & & \vdots & & \vdots \\ n_{1,q} & n_{2,q} & \cdots & n_{p,q} & \cdots & n_{K,q} \\ \vdots & \vdots & & \vdots & & \vdots \\ n_{1,2} & n_{2,2} & \cdots & n_{p,2} & \cdots & n_{K,2} \\ n_{1,1} & n_{2,1} & \cdots & n_{p,1} & \cdots & n_{K,1} \end{pmatrix} \equiv \begin{pmatrix} m_L \\ \vdots \\ m_q \\ \vdots \\ m_2 \\ m_1 \end{pmatrix}$$

Thus any basis state representing the configuration of particles on a 2D lattice with  $L$  rows can be thought of as a point in the  $L$ -dimensional hyper-space spanned by the row-states  $|\phi\rangle_m$  as shown in Fig.1. With these definitions, the number of possible

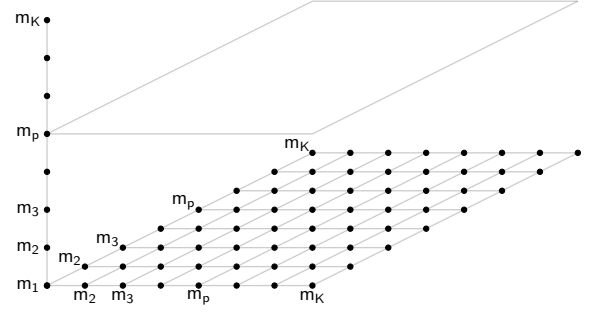


FIG. 1. For a lattice with 3 rows, any basis state can be identified as a point in the 3-dimensional space spanned by row-states.

basis states of the system is  $\alpha^L$ . Using these, any state of the system can be expressed in terms of the basis states as

$$|\psi\rangle = \sum_{M=0}^{\alpha^L-1} C^M |\Phi^L\rangle_M, \quad (11)$$

where  $C^M$  is the coefficient corresponding to the basis  $|\Phi^L\rangle_M$  in the wavefunction  $|\psi\rangle$ . The corresponding vector  $\mathbf{M} = (m_1, m_2, \dots, m_L)$  has the information regarding the occupancies along all the rows corresponding to  $M$ th basis state.

## B. Construction of Hamiltonian matrix

Let us now consider the BHM Hamiltonian given in Eq.1. Consider the hopping term  $-J\hat{b}_{p+1,q}^\dagger \hat{b}_{p,q}$  which describes the hopping of a particle from the lattice site  $(p, q)$  to  $(p+1, q)$ . The action of this term on a basis state affects only two lattice sites of the  $q$ th row. Thus, its operation on the row yields

$$\begin{aligned} &\hat{b}_{p+1,q}^\dagger \hat{b}_{p,q} |n_1, \dots, n_p, n_{p+1}, \dots, n_K\rangle \\ &= \sqrt{n_p (n_{p+1} + 1)} |n_1, \dots, (n_p - 1), (n_{p+1} + 1), \dots, n_K\rangle, \end{aligned}$$

if the hopping is allowed, which corresponds to  $n_p - 1 \geq 0$  and  $n_{p+1} \leq N_B - 1$ . Otherwise, the action of the hopping term results to zero. Thus for a possible hopping, this hopping term only modify the row-state  $|\phi\rangle_{m_q}$  to a different row-state  $|\phi\rangle_{m'_q}$

$$\hat{b}_{p+1,q}^\dagger \hat{b}_{p,q} |\phi\rangle_{m_q} = \sqrt{n_p (n_{p+1} + 1)} |\phi\rangle_{m'_q}, \quad (12)$$

and the quantum numbers of the two row-states are related as

$$\begin{aligned} m'_q - m_q &= \sum_{i=1}^K (n'_i - n_i) N_B^{i-1}, \\ &= N_B^{p-1} (N_B - 1). \end{aligned} \quad (13)$$

Thus, for a possible  $x$ -hopping, the operation of the hopping term  $-J\hat{b}_{p+1,q}^\dagger\hat{b}_{p,q}$  on the basis state  $|\Phi^L\rangle_M$  can be written as

$$-J\hat{b}_{p+1,q}^\dagger\hat{b}_{p,q}|\Phi^L\rangle_M = -J\sqrt{n_{p,q}(n_{p+1,q}+1)}|\Phi^L\rangle_{M'}, \quad (14)$$

where the corresponding basis states vectors  $\mathbf{M} = (m_1, m_2, \dots, m_L)$  and  $\mathbf{M}' = (m'_1, m'_2, \dots, m'_L)$  are related as

$$m'_i = \begin{cases} m_i & \text{if } i \neq q, \\ m_q + N_B^{p-1}(N_B - 1) & \text{if } i = q. \end{cases} \quad (15)$$

Here  $n_{p,q}$  is the occupancy at site  $(p, q)$  for the basis  $|\Phi^L\rangle_M$ . Thus we can calculate the non-zero matrix element of the hopping term as

$$\begin{aligned} (-J\hat{b}_{p+1,q}^\dagger\hat{b}_{p,q})_{M'M} &\equiv M' \langle \Phi^L | -J\hat{b}_{p+1,q}^\dagger\hat{b}_{p,q} | \Phi^L \rangle_M, \\ &= -J\sqrt{n_{p,q}(n_{p+1,q}+1)}. \end{aligned} \quad (16)$$

Similarly consider the hopping term  $-J\hat{b}_{p,q+1}^\dagger\hat{b}_{p,q}$  which describes the hopping of particles from lattice site  $(p, q)$  to  $(p, q+1)$  between two neighboring rows. The hopping term will modify the row-states at  $q+1$  and  $q$ th rows. Thus, for a possible  $y$ -hopping, the action of the hopping term  $-J\hat{b}_{p,q+1}^\dagger\hat{b}_{p,q}$  on the basis state  $|\Phi^L_M\rangle$  is given by

$$-J\hat{b}_{p,q+1}^\dagger\hat{b}_{p,q}|\Phi^L\rangle_M = -J\sqrt{n_{p,q}(n_{p,q+1}+1)}|\Phi^L\rangle_{M'}, \quad (17)$$

where,

$$m'_i = \begin{cases} m_i & \text{if } i \neq q, i \neq q+1, \\ m_q - N_B^p & \text{if } i = q, \\ m_{q+1} + N_B^p & \text{if } i = q+1. \end{cases} \quad (18)$$

and this contributes to the  $(M', M)$  Hamiltonian matrix element. In a similar way, the other terms of the Hamiltonian can be evaluated.

### III. STATE REDUCTION

The row-states  $|\phi\rangle_m$  and cluster-states  $|\Phi^q\rangle_M$  considered so far are without restrictions on the total number of particles  $N = \sum_{p=1}^K \sum_{q=1}^L n_{p,q}$  except for the constraint of  $n_{p,q}$  not exceeding  $N_B - 1$ . Thus, the basis states described by Eq.(10) includes all possible states with  $0 \leq N \leq (N_B - 1)^{KL}$ . Such a basis set is not appropriate for calculations with fixed  $N$  or for studies using the canonical ensemble. For such cases, let us refine the basis state construction to impose the constraint of selecting states with a particular value of  $N$ . This implies that  $n_{p,q}$  can range from 0 to  $\min(N, N_B)$ . Depending on the problem of interest, additional constraints can be imposed on basis states. For example, at unit filling ( $N = K \times L$ ) average occupancies at each lattice site is 1, thus basis states with occupancies  $n_{p,q} > 1$  may not contribute to the lowest energy sector. So it is appropriate to impose constraints which reduces the number of the basis states. These considerations, however, require modifications in the basis construction procedure and Hamiltonian matrix calculation.

$ n_1, n_2, n_3\rangle$	$m$	$j$
$ 1, 1, 0\rangle$	3	1
$ 1, 0, 1\rangle$	5	2
$ 0, 1, 1\rangle$	6	3
$ 1, 1, 1\rangle$	7	$\alpha = 4$

TABLE I. Identification of various possible row-state configurations with the corresponding values of the quantum number  $m$ .

#### A. Construction of the row-states

The single-site Fock states  $|n_{p,q}\rangle$  considered so far have occupancies  $0 \leq n_{p,q} \leq (N_B - 1)$ . For quantum states with higher average occupancies, it is appropriate to modify the choice of  $|n_{p,q}\rangle$  with the constraint

$$\eta \leq n_{p,q} \leq (\eta + N_B - 1). \quad (19)$$

This fixes the number of single-site Fock states to  $N_B$  but modifies the lowest possible occupancy of the single-site Fock state to  $\eta$ . The other constraint is to restrict the number of particles in a row state within a range of values

$$\sigma \leq \sum_{p=1}^K n_{p,q} \leq \sigma + \delta. \quad (20)$$

This sets a limit on the minimum number of particles in a row-state as  $\sigma$  and fixes the range to  $\delta$ . Such a constraint is appropriate to generate basis sets of optimal sizes to study quantum phases with low average occupancies. Further, as the constraint is on the range of  $N_m$ , it can also be imposed to limit the basis set size, but ensure that it represents the number fluctuation of the quantum phase appropriately. Thus, Eq.(4) can still be used to describe the row-states with the constraints in Eq.(19) and (20). Accordingly, the row-state quantum number is modified to

$$m = \sum_{p=1}^K (n_p - \eta) N_B^{p-1}. \quad (21)$$

To illustrate, as an example, consider a row consisting of 3 lattice sites and let us choose  $\eta = 0$ ,  $N_B = 2$ ,  $\sigma = 2$  and  $\sigma + \delta = 3$ . Table I shows the four possible row-state configurations, each uniquely identified by the row-state quantum number  $m$ . From the table it is evident that  $m$  does not vary uniformly, so to simplify we map  $m$  to a integer index  $j$  such that  $j = 1$  represents row-state with the lowest value of  $m$ . Then,  $j = 2$  corresponds to the row-state with the second lowest value of  $m$ , and so on as shown in Table I. In this way, we identify the  $j$ th row-state by the corresponding  $m$  value. As described earlier, the row-states are used to construct the basis for the entire system. The generation of the basis set is done by selecting states which satisfy the constraints considered earlier. This selection is simplified by the use of the multi-row states which forms the building block for the construction of the basis states.

### B. Multi-row states with constraints

The constraints as expressed in Eq. (19) and (20) are for the single-site and row-state, respectively. For the entire lattice system, a constraint on  $N$  can be imposed as

$$\Sigma \leq \sum_{p=1}^K \sum_{q=1}^L n_{p,q} \leq \Sigma + \Delta. \quad (22)$$

Like in the case of row-state, this sets a limit on the minimum number of particles in a basis state as  $\Sigma$  and fixes the range to  $\Delta$ . This constraint is suitable when total number of particles in the lattice is not fixed. Thus, to reduce the basis set to an optimal size but appropriate to describe the quantum phase of interest, constraints in Eq. (19), (20) and (22) are imposed to the single-site, row-state and basis state, respectively. It must however be mentioned that for studies with the Micro-canonical ensemble, the total number of particles is fixed and corresponds to  $\Delta = 0$ .

As described earlier, the multi-row states consisting of  $q$  rows are denoted by  $|\Phi^q\rangle_M$ , with a corresponding  $q$ -dimensional vector  $\mathbf{M}$  which identifies the row-states in the  $q$  rows. The two-row cluster-states can be constructed as a direct product of two row-states  $|\phi\rangle_{m_1}$  and  $|\phi\rangle_{m_2}$  as

$$|\Phi^2\rangle_M \equiv |\phi\rangle_{m_1} \otimes |\phi\rangle_{m_2} : N_M \leq \Sigma + \Delta \quad (23)$$

Here,  $\mathbf{M} = (m_1, m_2)$  has the row-state quantum numbers of the two contributing row-states satisfying the constraint that total number of particles in the two-row state can at-most be equal to  $\Sigma + \Delta$ . The Table II lists the possible two-row states for  $N = 4$  generated from the row-states in Table I. Each of the two-row states is associated with an index  $j \in \{1, 2, \dots, \alpha^{(2)}\}$ , where  $\alpha^{(2)}$  is the total number of possible two-row states. The sequence of the two-row states is defined in accordance with the quantum numbers of the two contributing row-states. As shown in Table II, the two-row states are sequenced in terms the pair of quantum numbers as  $(m_1, m_2)$ , with the left as the fast varying. This definition is consistent with Eq. (8). Due to the constraints the basis states, however, cannot be identified with quantum number  $M$  as given in Eq. (8). To identify each of the basis states, an index  $j$  is assigned according to the ordered sequence. Here, with the imposition of the constraints in Eq.(22), it is to be noted that  $\alpha^{(2)} \leq (\alpha)^2$ .

Similarly the three-row states can be constructed as a direct product of two-row state with label  $M$  and a row-state with quantum number  $m$  as

$$|\Phi^3\rangle_{M'} \equiv |\Phi^2\rangle_M \otimes |\phi\rangle_m : N_{M'} \leq \Sigma + \Delta. \quad (24)$$

Here,  $M'$  is a vector containing the information of the row-state configurations. An index  $j \in \{1, 2, \dots, \alpha^{(3)}\}$  uniquely identifies each of the three-row states. Following similar steps, states with larger number of row states can be constructed.

$ \Phi^2\rangle_M = \begin{pmatrix} n'_1, n'_2, n'_3 \\ n_1, n_2, n_3 \end{pmatrix}$	$\mathbf{M} = (m_1, m_2)$	$j$
$\begin{pmatrix} 1, 1, 0 \\ 1, 1, 0 \end{pmatrix}$	(3, 3)	1
$\begin{pmatrix} 1, 0, 1 \\ 1, 1, 0 \end{pmatrix}$	(5, 3)	2
$\begin{pmatrix} 0, 1, 1 \\ 1, 1, 0 \end{pmatrix}$	(6, 3)	3
$\begin{pmatrix} 1, 1, 0 \\ 1, 0, 1 \end{pmatrix}$	(3, 5)	4
$\begin{pmatrix} 1, 0, 1 \\ 1, 0, 1 \end{pmatrix}$	(5, 5)	5
$\begin{pmatrix} 0, 1, 1 \\ 1, 0, 1 \end{pmatrix}$	(6, 5)	6
$\begin{pmatrix} 1, 1, 0 \\ 0, 1, 1 \end{pmatrix}$	(3, 6)	7
$\begin{pmatrix} 1, 0, 1 \\ 0, 1, 1 \end{pmatrix}$	(5, 6)	8
$\begin{pmatrix} 0, 1, 1 \\ 0, 1, 1 \end{pmatrix}$	(6, 6)	$\alpha^{(2)} = 9$

TABLE II. Various possible two-row cluster-states and corresponding vector label  $\mathbf{M}$  for atmost 4 particles within the cluster of 2 rows.

### C. Basis states with constraints

To generate the basis states for the entire lattice system with the constraints, we again use the multi-row states as the building blocks. In short, the basis states can be a multi-row state or product of two multi-row states with appropriate number of rows. However, only the basis states satisfying the constraint in Eq. (22) are selected. Consider the case of  $L = 3$  as an example. The basis states which satisfy the constraint in Eq. (22) are to be selected from the set  $\{|\Phi^3\rangle_M\}$ , and the members of this set are generated with the constraints in Eq. (19), (20) and (23). Let

$$|\Phi^3\rangle_{M'} \equiv |\Phi^3\rangle_j \in \{|\Phi^3\rangle_M\} : \Sigma \leq N_{M'} \leq \Sigma + \Delta, \quad (25)$$

be one of the three-row states which satisfies all the constraints. Here  $N_{M'}$  represents total number of particles in the cluster-state. Then, the collection of these states forms the desired basis set  $\{|\Phi^3\rangle_{M'}\}$ . To identify the states uniquely, each of the state is assigned an integer index  $j \in \{1, 2, \dots, \beta\}$ , where  $\beta$  is the total number of states in  $\{|\Phi^3\rangle_{M'}\}$  with  $\beta \leq \alpha^{(3)}$ . Similarly, for the case of a larger lattice  $L = 5$ , we can use the three- and two-row states to generate basis states as

$$|\Phi^L\rangle_j = |\Phi^{L_1}\rangle_{M_1} \otimes |\Phi^{L_2}\rangle_{M_2} : \Sigma \leq N_j = N_{M_1} + N_{M_2} \leq \Sigma + \Delta, \quad (26)$$

where,  $L = 5$ ,  $L_1 = 3$ , and  $L_2 = 2$ . Once  $\{|\Phi^L\rangle_j\}$  is generated, the model Hamiltonian can then be diagonalized to obtain the ground state as a linear combination

$$|\Psi\rangle = \sum_{j=1}^{\beta} C^j |\Phi^L\rangle_j, \quad (27)$$

where  $C^j$  is the coefficient corresponding to the contribution of the basis  $|\Phi^L\rangle_j$ .

### D. Calculation of Hamiltonian matrix elements

Consider the BHM Hamiltonian in Eq. (1), and as an example select one of the hopping terms  $-\hat{J} \hat{b}_{p+1,q}^\dagger \hat{b}_{p,q}$ . Then,

$j$	$(m_1, \dots, m_{L-1}, m_L)$
1	$(\tilde{m}_1, \dots, \tilde{m}_1, \tilde{m}_1)$
2	$(\tilde{m}_2, \dots, \tilde{m}_1, \tilde{m}_1)$
$\vdots$	$\vdots \quad \vdots \quad \vdots$
$j_1$	$(\tilde{m}_\alpha, \dots, \tilde{m}_1, \tilde{m}_1)$
$j_1 + 1$	$(\tilde{m}_1, \dots, \tilde{m}_2, \tilde{m}_1)$
$j_1 + 2$	$(\tilde{m}_2, \dots, \tilde{m}_2, \tilde{m}_1)$
$\vdots$	$\vdots \quad \vdots \quad \vdots$
$j_2$	$(\tilde{m}_\alpha, \dots, \tilde{m}_2, \tilde{m}_1)$
$\vdots$	$\vdots \quad \vdots \quad \vdots$
$j_3$	$(\tilde{m}_\alpha, \dots, \tilde{m}_\alpha, \tilde{m}_1)$
$j_3 + 1$	$(\tilde{m}_1, \dots, \tilde{m}_1, \tilde{m}_2)$
$\vdots$	$\vdots \quad \vdots \quad \vdots$
$j_4$	$(\tilde{m}_\alpha, \dots, \tilde{m}_\alpha, \tilde{m}_2)$
$\vdots$	$\vdots \quad \vdots \quad \vdots$
$\beta$	$(\tilde{m}_\alpha, \dots, \tilde{m}_\alpha, \tilde{m}_\alpha)$

TABLE III. Table showing the labels  $m_q$  of the row-state configurations, along various rows, that together constitute the  $j$ th basis state. Here, the row-state labels  $\tilde{m}_q$  satisfy  $\tilde{m}_1 < \tilde{m}_2 < \dots < \tilde{m}_\alpha$ .

it's operation on the row- and basis states can be evaluated using the expressions in Eq.(12-15). For the  $j$ th basis state with row-state components given by vector  $\mathbf{R}$ , we get

$$-J\hat{b}_{p+1,q}^\dagger \hat{b}_{p,q} |\Phi^L\rangle_R = -J\sqrt{n_{p,q}(n_{p+1,q} + 1)} |\Phi^L\rangle_{R'}. \quad (28)$$

Here, both the states  $|\Phi^L\rangle_R$ , and  $|\Phi^L\rangle_{R'}$  are members of the basis set  $\{|\Phi^L\rangle_{M'}\}$  obtained with the constraints. From earlier considerations, the row-state quantum numbers of the two basis states  $\mathbf{R} = (r_1, r_2, \dots, r_L)$  and  $\mathbf{R}' = (r'_1, r'_2, \dots, r'_L)$  are related by  $r'_i = r_i$  for  $i \neq q$  and  $r'_q = r_q + N_B^{p-1}(N_B - 1)$ . This uniquely identifies  $\mathbf{R}'$  but the corresponding identification index of  $|\Phi^L\rangle_{R'}$  is yet unknown as the relation in Eq. (8) is not applicable due to state reduction. Once the identification indices are known we can define the Hamiltonian matrix  $H_{jk} = {}_{R'}\langle \Phi^L | H_{\text{BHM}} | \Phi^L \rangle_R$  and continue the process for all the hopping terms in the BHM Hamiltonian to generate the Hamiltonian matrix.

### E. Identifying the basis index $j$ of $\mathbf{R}'$

As mentioned earlier, for the  $j$ th basis state  $|\Phi^L\rangle_j$  the corresponding vector label  $\mathbf{M} = (m_1, m_2, \dots, m_L)$  contains the row-state quantum numbers of the constituent rows. This forms a forward map between the basis state index  $j$  and row-state configurations contained in the vector label  $\mathbf{M}$

$$|\Phi^L\rangle_j \rightarrow |\phi\rangle_{m_1} \otimes |\phi\rangle_{m_2} \cdots \otimes |\phi\rangle_{m_L}. \quad (29)$$

However, we also require the inverse map. As we had discussed earlier, the calculation of the Hamiltonian matrix re-

quire the information of the basis state index  $j$  corresponding to a given configuration of row-state quantum numbers or  $\mathbf{M}$ . This can be resolved using the structure adopted while constructing the basis set. We recall that the number of possible row-state configurations is  $\alpha$  and each row-state is identified with a positive integer label  $m$ . To aid in calculations, the row-states are sequenced in ascending order of  $m$ . Using this notation, the identifying vector  $\mathbf{M}$  is defined such that the left (right) most component is the fast (slow) varying index. That is, the basis states  $|\Phi^L\rangle_j$  are identified and sequenced in terms of row-state quantum numbers  $(m_1, m_2, \dots, m_L)$ , where the index  $m_q$  vary faster than the  $m_{q+1}$  with  $j$ . As an example, the sequence of the row-state labels for the basis states are shown in shown in Table III.

Let us suppose that we have a basis state with row-state configuration  $\mathbf{R}' = (r'_1, r'_2, \dots, r'_L)$  and have to identify the corresponding state index  $j$  from the basis set. To accomplish this, we perform a search using the method of bisection in the interval  $j \in [1, \beta]$ . Considering that the rightmost index is slowest varying, we start the bisection to identify the range of basis set index  $j \in [j_{\min}^L, j_{\max}^L]$  which has  $r'_L$  as the rightmost row-state index within the basis set. Next, a bisection search is done within the range  $[j_{\min}^L, j_{\max}^L]$  to locate the range  $[j_{\min}^{L-1}, j_{\max}^{L-1}]$  which lies within  $[j_{\min}^L, j_{\max}^L]$  and has row-state  $r'_{L-1}$ . At this stage all the basis states within the range  $[j_{\min}^{L-1}, j_{\max}^{L-1}]$  have the same row-states  $r'_L$  and  $r'_{L-1}$  as the desired state  $\mathbf{R}'$ . We continue the bisection further for each of the row-state index and the required  $j$  is obtained in the last bisection with the identification of the  $r'_1$ . Thus the inverse map needed for locating the basis index from row-state configurations can be achieved through a sequence of  $L$  bisection searches. It should be noted that each bisection search requires a maximum of  $\ln_2(\beta)$  comparisons of the row-state quantum number.

Using this method we can, then, generate the Hamiltonian matrix similar to the approach described in Section II B. For a state  $|\Phi^L\rangle_j$ , we identify the  $j'$   $\langle \Phi^L |$  which has non-zero matrix element for each of the terms in the Hamiltonian and calculate the matrix element. This generates the Hamiltonian matrix elements along the column corresponding to  $j'$   $\langle \Phi^L |$ . Continuing the process for other states, the Hamiltonian matrix can be calculated column wise.

## IV. ENTANGLEMENT IN THE QUANTUM PHASE

The topological characteristics of a system can be inferred by studying the entanglement in the system. It can be used to distinguish a topologically ordered phase like quantum Hall from a normal phase like superfluid. Among various indicators of entanglement in a system, the bipartite entanglement entropy is considered robust. In real-space, it is calculated by partitioning the lattice system into two sub-systems, say, A and B. The many-body ground-state wavefunction of the system can then be written in a Schmidt decomposed form as

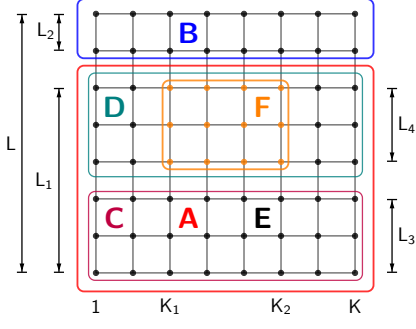


FIG. 2. Visual illustration for the bipartition of the lattice for obtaining the reduced density matrix of sub-system F. First, the lattice is partitioned along the  $y$ -axis into sub-systems A and B. Then, sub-system A is further sub-divided into sub-systems C and D. Finally, sub-system D is partitioned along the  $x$  axis to give the sub-system F. The boundary of the sub-systems are identifiable from the corresponding color of the sub-system label. The sub-system E corresponding to the surrounding of sub-system F constitutes the black colored lattice sites.

[41]

$$|\Psi\rangle = \sum_i \sqrt{\lambda_i} |\Psi_A\rangle \otimes |\Psi_B\rangle. \quad (30)$$

Here,  $\lambda_i$  are the Schmidt coefficients and these are the eigenvalues of the reduced density matrix of the sub-system. The reduced density matrix associated with sub-system A can be obtained from the density matrix after tracing over the degrees of freedom associated with the sub-system B,  $\rho_A = \text{Tr}_B |\Psi\rangle \langle \Psi|$ . The eigenvalues  $\lambda_i$  of the reduced density matrix give the entanglement spectra and the bi-partite entanglement entropy of the system is the Von Neumann entropy associated with the reduced density matrix,

$$S_E = -\text{Tr}[\rho_A \log \rho_A] = -\sum_i \lambda_i \log \lambda_i. \quad (31)$$

The entanglement entropy  $S_E$  scales with the length ( $L$ ) of the interface between the two sub-systems as [32, 33]

$$S_E = \alpha L - \gamma + \mathcal{O}(L^{-\nu}), \quad \nu > 0, \quad (32)$$

where  $-\gamma$  is the topological entanglement entropy. It measures the quantum dimension of the quasiparticle excitations in the FQH states. The topologically ordered  $\nu = 1/m$  FQH state has  $\gamma = 1/2 \log(m)$ . The Area-law scaling of the entanglement is typical of ground states for gapped systems [42].

### A. Constructing bipartite reduced density matrix

The approach adopted in the construction of the basis set can be employed in an optimal way to calculate the bipartite reduced density matrix. For this consider partitioning a lattice system with  $L$  rows into two subsystems A and B, such that

the sub-system A consists of bottom  $L_1$  rows and B consists of top  $L_2 = L - L_1$  rows. This is shown schematically in Fig. 2. As each basis state of the lattice consists of  $L$  row states, and following Eq. (26) we can write

$$|\Phi^L\rangle_M \equiv |\Phi^{L_1}\rangle_{M_1} \otimes |\Phi^{L_2}\rangle_{M_2} : \Sigma \leq N_{M_1} + N_{M_2} \leq \Sigma + \Delta. \quad (33)$$

Each basis state  $|\Phi^L\rangle_M$ , labelled with index  $j$ , is thus the direct product of multi-row states  $|\Phi^{L_1}\rangle_{M_1}$  and  $|\Phi^{L_2}\rangle_{M_2}$  with labels  $j_1$  and  $j_2$ , respectively. The reduced density matrix  $\rho_A$  would then be a  $\alpha^{(L_1)}$  dimensional matrix and is obtained after tracing over the degrees of freedom associated with  $j_2$

$$\begin{aligned} \rho_A(k, l) &= \sum_{j=1}^{\beta} \sum_{j'=1}^{\beta} C^{*j} C^{j'} \delta_{j_2, j'_2} \delta_{j_1, k} \delta_{j'_1, l} \\ &= \sum_{j=1}^{\beta} \sum_{j'=1}^{\beta} \rho(j, j') \delta_{j_2, j'_2} \delta_{j_1, k} \delta_{j'_1, l}. \end{aligned} \quad (34)$$

Here  $\rho = |\Psi\rangle \langle \Psi|$  is the density matrix of the system. Similarly the sub-system A can be further partitioned into two sub-systems C and D consisting of bottom  $L_3$  rows and top  $L_4 = L_1 - L_3$  rows, respectively. Thus the sub-system state  $|\Phi^{L_1}\rangle_M$ , labelled with index  $j$  for  $1 \leq j \leq \alpha^{(L_1)}$ , is the direct product of the state of sub-systems C  $|\Phi^{L_3}\rangle_{M_3}$  and D  $|\Phi^{L_4}\rangle_{M_4}$  with corresponding indexes  $1 \leq j_3 \leq \alpha^{(L_3)}$  and  $1 \leq j_4 \leq \alpha^{(L_4)}$ , respectively. Thus the  $\alpha^{(L_4)}$  dimensional reduced density matrix  $\rho_D$  can be obtained as

$$\rho_D(k, l) = \sum_{j=1}^{\alpha^{(L_1)}} \sum_{j'=1}^{\alpha^{(L_1)}} \rho_A(j, j') \delta_{j_3, j'_3} \delta_{j_4, k} \delta_{j'_4, l}. \quad (35)$$

The bi-partitioning of the system discussed so far is by separating along the rows. An example of the partition geometry is as indicated by the sublattices A and B in Fig. 2. However, following ref. [32] the calculation of entanglement entropy requires bi-partitioning the system into an isolated and surrounding domains. This is as indicated by the subsystem F and the remaining part E in Fig. 2. In the figure, the orange colored lattice sites constitute the sub-system F and the rest of lattice sites in black constitute the subsystem E. The orange boundary marks the bi-partite separation between sub-systems F and E. In this case, the partitioning involves both along rows and columns. To describe the partitioning with a specific example, consider the subdivision of the whole system in Fig. 2 into two, the isolated region F and the remaining part E. To calculate the reduced density matrix of the sub-system F, first the subsystems B and C can be traced out using the method discussed earlier. Then, the required reduced density matrix is obtained by partitioning sub-system D into sub-system F and the remaining lattice sites which forms a part of the sub-system E as shown in Fig. 2. The surrounding of subsystem F corresponds to black-colored lattice sites which constitutes the subsystem E. The partitioning involves tracing out columns on the left and right of subsystem F. Thus, the lattice sites  $(p, q)$  for which  $L_3 \leq q \leq L_1$  and

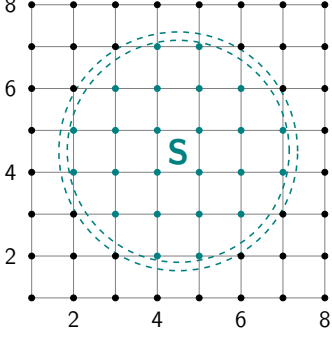


FIG. 3. Visual illustration for spatial bi-partitioning of the lattice such that the lattice sites within the circle (teal colored sites) are chosen as a part of the sub-system  $S$ .

$p \in \{K_1, K_1 + 1, \dots, p, \dots, K_2\}$  lie in sub-system  $F$  and rest of sites are a part of sub-system  $E$  over which we wish to trace out. This necessitates the introduction of a unique label corresponding to the different configuration of particles in sub-system  $F$ . If the total number of sites in the subsystem  $F$  is not large, we can use the following scheme for assigning each configuration with a unique label  $m$  given by

$$m = \sum_{q=L_3+1}^{L_1} \sum_{p=K_1}^{K_2} (n_{p,q} - \eta) N_B^{(p-K_1)+(L_1-q)(K_2-K_1+1)}. \quad (36)$$

Since, for each multi-row state  $j$  of sub-system  $D$ , configuration of particles in the sub-system  $F$  corresponds to label  $m_j$  given by Eq.(36). Thus, the reduced density matrix of sub-system  $F$  can be expressed as

$$\rho_F(k, l) = \sum_{j=1}^{\alpha(L_4)} \sum_{j'=1}^{\alpha(L_4)} \rho_D(j, j') \delta_{m_j, k} \delta_{m_{j'}, l} \prod_{p,q} \delta_{n_{p,q}, n'_{p,q}}, \quad (37)$$

where  $n_{p,q}$  and  $n'_{p,q}$  are occupancies at the lattice site  $(p, q)$  corresponding to the multi-row states with indexes  $j$  and  $j'$ , respectively. And, the prime on the product over lattice sites  $(p, q)$  signifies that product is restricted over only those lattice sites for which  $p \in \{1, 2, \dots, K_1 - 1, K_2 + 1, \dots, K\}$  and  $q \in \{L_3 + 1, L_3 + 2, \dots, L_1\}$ . Alternatively, if the total number of lattice sites in sub-system  $F$  is large then instead of assigning a label to each configuration using Eq.(36), we can construct the multi-row states using rowstates of  $K_2 - K_1$  lattice site. And, each configuration of particles in sub-system  $F$  can then be uniquely identified with the multi-row index described earlier.

## B. Fractional quantum Hall on a lattice

The topological entanglement entropy  $\gamma$  is an appropriate property to distinguish quantum Hall states from the other competing states which are not topological in nature. As an application of the scheme we have developed, we consider the

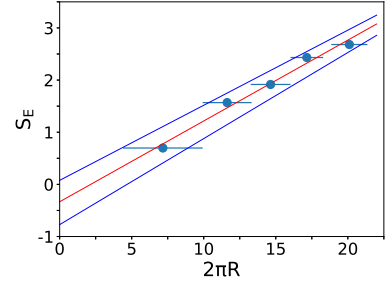


FIG. 4. Entanglement entropy ( $S_E$ ) of the sub-system  $S$  as a function of the length  $2\pi R$  of the circular boundary separating  $S$  from the rest of the lattice. The  $x$ -error bars represents the ambiguity in the definition of boundary length.

FQH state on a square lattice. The FQH states are supported in optical lattice with the introduction of synthetic magnetic fields. With this, the hopping term of BHM acquires a lattice-site dependent Peierls phase. The Hamiltonian of the system in the Landau gauge is given by [43]

$$\hat{H} = \sum_{p,q} \left[ \left( -J e^{i2\pi\alpha} \hat{b}_{p+1,q}^\dagger \hat{b}_{p,q} - J \hat{b}_{p,q+1}^\dagger \hat{b}_{p,q} + \text{H.c.} \right) + \frac{U}{2} \hat{n}_{p,q} (\hat{n}_{p,q} - 1) - \mu \hat{n}_{p,q} \right], \quad (38)$$

where,  $\alpha$  corresponds to the the strength of the magnetic field. We obtain the  $\nu = 1/2$  FQH state for a system of 4 hardcore bosons on a  $8 \times 8$  lattice with periodic boundary conditions and synthetic magnetic field  $\alpha = 1/8$ . We find the ground state is doubly degenerate, which is an essential property of  $\nu = 1/2$  FQH state on a torus geometry [44]. Using the prescription of Hatsugai [45], we have verified the topological nature of the state and find the many-body Chern number is 1. To calculate  $\gamma$ , we bi-partition the lattice system as schematically shown in Fig.3. Then, we calculate  $\gamma$  between the subsystem  $S$  and the rest of the lattice. However, as the lattice is discrete in nature, bi-partitioning it with circular geometry introduces an ambiguity in the definition of the boundary as shown in Fig.3. So, for a given configuration of lattice sites in the subsystem  $S$ , we can consider the boundary of the circle enclosing  $S$  to lie within the minimum and maximum radii ( $R_{\min}, R_{\max}$ ). The scaling of  $S_E$  with the boundary length  $L$ , as shown in Fig.4, are bounded by two lines, the lower and upper lines corresponding to least square fit of data for circles with radii  $R_{\min}$  and  $R_{\max}$ , respectively. In the figure, the least square fit with the average of the two radii is represented by the middle line. We observe that  $\gamma$ , which is the  $y$ -intercept, depends on the chosen definition of the boundary length and varies from 0.08 to  $-0.77$ . Considering the average value of the radius  $(R_{\min} + R_{\max})/2$ , and a least square fit, shown as the middle line in Fig.4 gives  $\gamma = 0.33 \pm 0.17$ . This value is consistent with the theoretical estimate of  $\gamma = \ln\sqrt{2} \approx 0.347$  for a  $\nu = 1/2$  abelian FQH state. The numerical estimates can be improved by incorporating entropy calculations with larger values of  $L$  which needs a larger lattice dimensions, however,

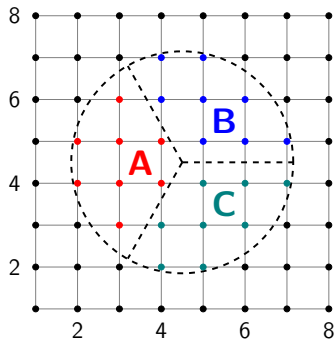


FIG. 5. Visual illustration for spatial bi-partitioning of the subsystem in three slices, forming the plural areas. The lattice sites in each subsystem are color coded corresponding to the color of the subsystem label.

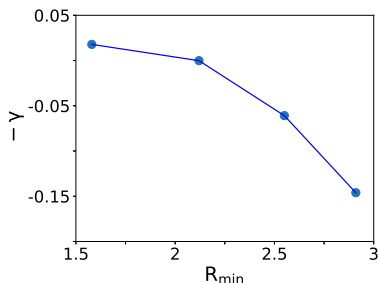


FIG. 6. Topological entanglement entropy ( $-\gamma$ ) calculated with various choices of the circular subsystem  $S$  against the radius  $R_{\min}$ .

the ambiguity in the definition of  $L$  would still be present.

Using the prescription of Kitaev and Preskill for the calculation  $\gamma$  in terms of the multiple areas, it can be calculated without the ambiguity of boundary length. In their method  $\gamma$  is given by an appropriate combination of the entanglement entropies of the multiple areas of the subsystem  $S$  (shown in Fig.5) according to the relation  $S_{ABC} - S_{AB} - S_{BC} - S_{AC} + S_A + S_B + S_C = -\gamma$  [32]. With this formulation, we have calculated the  $\gamma$  for various sizes of sub-system  $S$  and the results are shown in Fig.6. We observe that the numerical estimates of the  $\gamma$  is different from the theoretical estimate of  $-0.35$ . However, the calculated  $\gamma$  improves with the larger dimensions of the sub-system  $S$ . This can be due to the requirement of a smooth large sized boundary compared to the

correlation length  $\xi \ll R$ . The estimates of  $\gamma$  can be improved with a larger sized subsystem on a larger lattice but the computational resources required is beyond the scope of accessible computational resources.

## V. DISCUSSIONS

We report the development of a new method on exact diagonalization. It relies on a hierarchy of states to define the basis states of a lattice system. The starting point is the Fock states of the single lattice sites. Using these, row-states are defined as direct product and then, the product of the row-states form the cluster-states. The approach is flexible and it is particularly well suited for studying bosonic optical lattice systems. For such a system, there is no limit on the lattice site occupancy, and the number of basis states grows very fast with the system size and number of particles. In this multi-step and hierarchical approach, we can impose various constraints to restrict on the basis set and this offers an advantage in optimizing the size of the Hamiltonian matrix. The generation of the Hamiltonian matrix is also optimized by identifying the pairs of states which has non-zero matrix elements. For the case of the calculations with constraints, we use bisection method to accelerate the identification and calculation of the non-zero Hamiltonian matrix elements. All of the constituent steps are parallelizable. In our implementation we have parallelized both the basis set generation and calculation of the Hamiltonian matrix elements. Further more, we parallelize the diagonalization of the Hamiltonian matrix using PARPACK [46]. Using the method, we show how to partition a lattice system, compute the reduced density matrix and calculate the topological entanglement entropy. This is applied to the  $\nu = 1/2$  FQH state.

## VI. ACKNOWLEDGEMENTS

The results presented in this paper were computed on Vikram-100, the 100TFLOP HPC cluster and Param Vikram-1000 HPC cluster at Physical Research laboratory, Ahmedabad, India. We thank Dr. Rukmani Bai and Dr. Soumik Bandyopadhyay for useful discussions. DA would like to acknowledge support from the Science and Engineering Research Board, Department of Science and Technology, Government of India through Project No. CRG/2022/007099 and support from the UGC through the SAP (DRS-II), Department of Physics, Manipur University.

- 
- [1] P. M. Chaikin and T. C. Lubensky, *Principles of Condensed Matter Physics* (Cambridge University Press, 1995).  
 [2] Anders W. Sandvik and Juhani Kurkijärvi, “Quantum monte carlo simulation method for spin systems,” *Phys. Rev. B* **43**, 5950–5961 (1991).  
 [3] A W Sandvik, “A generalization of handscomb’s quantum monte carlo scheme-application to the 1d hubbard model,”

- Journal of Physics A: Mathematical and General* **25**, 3667 (1992).  
 [4] Patrik Henelius and Anders W. Sandvik, “Sign problem in monte carlo simulations of frustrated quantum spin systems,” *Phys. Rev. B* **62**, 1102–1113 (2000).  
 [5] Cornelius Lanczos, “Solution of systems of linear equations by minimized iterations,” *J. Res. Nat. Bur. Standards* **49**, 33–53

- (1952).
- [6] D. Calvetti, L. Reichel, and D. C. Sorensen, “An implicitly restarted lanczos method for large symmetric eigenvalue problems,” *Electron. Trans. Numer. Anal.* **2**, 1–21 (1994).
- [7] Andreas M. Läuchli, Julien Sudan, and Erik S. Sørensen, “Ground-state energy and spin gap of spin- $\frac{1}{2}$  kagomé-heisenberg antiferromagnetic clusters: Large-scale exact diagonalization results,” *Phys. Rev. B* **83**, 212401 (2011).
- [8] Andreas M. Läuchli, Julien Sudan, and Roderich Moessner, “ $s = \frac{1}{2}$  kagome heisenberg antiferromagnet revisited,” *Phys. Rev. B* **100**, 155142 (2019).
- [9] Rukmani Bai, Soumik Bandyopadhyay, Sukla Pal, K. Suthar, and D. Angom, “Bosonic quantum hall states in single-layer two-dimensional optical lattices,” *Phys. Rev. A* **98**, 023606 (2018).
- [10] Anders W. Sandvik, “Computational Studies of Quantum Spin Systems,” *AIP Conference Proceedings* **1297**, 135–338 (2010), [https://pubs.aip.org/aip/acp/article-pdf/1297/1/135/11407753/135\\_1\\_online.pdf](https://pubs.aip.org/aip/acp/article-pdf/1297/1/135/11407753/135_1_online.pdf).
- [11] Alexander Wietek and Andreas M. Läuchli, “Sublattice coding algorithm and distributed memory parallelization for large-scale exact diagonalizations of quantum many-body systems,” *Phys. Rev. E* **98**, 033309 (2018).
- [12] Jung-Hoon Jung and Jae Dong Noh, “Guide to exact diagonalization study of quantum thermalization,” *Journal of the Korean Physical Society* **76**, 670–683 (2020).
- [13] Maciej Lewenstein, Anna Sanpera, and Verònica Ahufinger, *Ultracold Atoms in Optical Lattices: Simulating quantum many-body systems* (Oxford University Press, 2012).
- [14] M. Greiner, O. Mandel, T. Esslinger, T. W. Hänsch, and I. Bloch, “Quantum phase transition from a superfluid to a Mott insulator in a gas of ultracold atoms,” *Nature (London)* **415**, 39 (2002).
- [15] M. Lewenstein, A. Sanpera, V. Ahufinger, B. Damski, A. Sen(De), and U. Sen, “Ultracold atomic gases in optical lattices: mimicking condensed matter physics and beyond,” *Adv. Phys.* **56**, 243 (2007).
- [16] J. Hubbard, “Electron correlations in narrow energy bands,” *Proc. Royal Soc. A* **276**, 238 (1963).
- [17] M. P. A. Fisher, P. B. Weichman, G. Grinstein, and D. S. Fisher, “Boson localization and the superfluid-insulator transition,” *Phys. Rev. B* **40**, 546 (1989).
- [18] D. Jaksch, C. Bruder, J. I. Cirac, C. W. Gardiner, and P. Zoller, “Cold bosonic atoms in optical lattices,” *Phys. Rev. Lett.* **81**, 3108 (1998).
- [19] D. S. Rokhsar and B. G. Kotliar, “Gutzwiller projection for bosons,” *Phys. Rev. B* **44**, 10328 (1991).
- [20] K. Sheshadri, H. R. Krishnamurthy, R. Pandit, and T. V. Ramakrishnan, “Superfluid and insulating phases in an interacting-boson model: Mean-field theory and the RPA,” *EPL* **22**, 257 (1993).
- [21] M. Ö. Oktel, M. Nišić, and B. Tanatar, “Mean-field theory for Bose-Hubbard model under a magnetic field,” *Phys. Rev. B* **75**, 045133 (2007).
- [22] J M Zhang and R X Dong, “Exact diagonalization: the bose-hubbard model as an example,” *Eur. J. Phys.* **31**, 591 (2010).
- [23] David Raventós, Tobias Graß, Maciej Lewenstein, and Bruno Juliá-Díaz, “Cold bosons in optical lattices: a tutorial for exact diagonalization,” *J. Phys. B* **50**, 113001 (2017).
- [24] M. Aidelsburger, M. Atala, S. Nascimbène, S. Trotzky, Y.-A. Chen, and I. Bloch, “Experimental realization of strong effective magnetic fields in an optical lattice,” *Phys. Rev. Lett.* **107**, 255301 (2011).
- [25] M. Aidelsburger, M. Atala, M. Lohse, J. T. Barreiro, B. Paredes, and I. Bloch, “Realization of the Hofstadter Hamiltonian with ultracold atoms in optical lattices,” *Phys. Rev. Lett.* **111**, 185301 (2013).
- [26] K. Jiménez-García, L. J. LeBlanc, R. A. Williams, M. C. Beeler, A. R. Perry, and I. B. Spielman, “Peierls substitution in an engineered lattice potential,” *Phys. Rev. Lett.* **108**, 225303 (2012).
- [27] Jean Dalibard, Fabrice Gerbier, Gediminas Juzeliūnas, and Patrik Öhberg, “Colloquium: Artificial gauge potentials for neutral atoms,” *Rev. Mod. Phys.* **83**, 1523–1543 (2011).
- [28] M Aidelsburger, “Artificial gauge fields and topology with ultracold atoms in optical lattices,” *Journal of Physics B: Atomic, Molecular and Optical Physics* **51**, 193001 (2018).
- [29] N. R. Cooper, J. Dalibard, and I. B. Spielman, “Topological bands for ultracold atoms,” *Rev. Mod. Phys.* **91**, 015005 (2019).
- [30] Philipp Hauke and Iacopo Carusotto, “Quantum hall and synthetic magnetic-field effects in ultra-cold atomic systems,” (2022).
- [31] Julian Léonard, Sooshin Kim, Joyce Kwan, Perrin Segura, Fabian Grusdt, Cécile Repellin, Nathan Goldman, and Markus Greiner, “Realization of a fractional quantum hall state with ultracold atoms,” *Nature* **619**, 495–499 (2023).
- [32] Alexei Kitaev and John Preskill, “Topological entanglement entropy,” *Phys. Rev. Lett.* **96**, 110404 (2006).
- [33] Michael Levin and Xiao-Gang Wen, “Detecting topological order in a ground state wave function,” *Phys. Rev. Lett.* **96**, 110405 (2006).
- [34] Hui Li and F. D. M. Haldane, “Entanglement spectrum as a generalization of entanglement entropy: Identification of topological order in non-abelian fractional quantum hall effect states,” *Phys. Rev. Lett.* **101**, 010504 (2008).
- [35] J. C. Budich, J. Eisert, and E. J. Bergholtz, “Topological insulators with arbitrarily tunable entanglement,” *Phys. Rev. B* **89**, 195120 (2014).
- [36] Maria Hermanns, Yann Salimi, Masudul Haque, and Lars Fritz, “Entanglement spectrum and entanglement hamiltonian of a chern insulator with open boundaries,” *Journal of Statistical Mechanics: Theory and Experiment* **2014**, P10030 (2014).
- [37] Alejandro José Uría-Álvarez, Daniel Molpeceres-Mingo, and Juan José Palacios, “Deep learning for disordered topological insulators through their entanglement spectrum,” *Phys. Rev. B* **105**, 155128 (2022).
- [38] Bela Bauer and Chetan Nayak, “Area laws in a many-body localized state and its implications for topological order,” *Journal of Statistical Mechanics: Theory and Experiment* **2013**, P09005 (2013).
- [39] Maksym Serbyn, Z. Papić, and Dmitry A. Abanin, “Universal slow growth of entanglement in interacting strongly disordered systems,” *Phys. Rev. Lett.* **110**, 260601 (2013).
- [40] Maksym Serbyn, Alexios A. Michailidis, Dmitry A. Abanin, and Z. Papić, “Power-law entanglement spectrum in many-body localized phases,” *Phys. Rev. Lett.* **117**, 160601 (2016).
- [41] Artur Ekert and Peter L. Knight, “Entangled quantum systems and the Schmidt decomposition,” *American Journal of Physics* **63**, 415–423 (1995), [https://pubs.aip.org/aapt/ajp/article-pdf/63/5/415/11806926/415\\_1\\_online.pdf](https://pubs.aip.org/aapt/ajp/article-pdf/63/5/415/11806926/415_1_online.pdf).
- [42] J. Eisert, M. Cramer, and M. B. Plenio, “Colloquium: Area laws for the entanglement entropy,” *Rev. Mod. Phys.* **82**, 277–306 (2010).
- [43] D. Jaksch and P. Zoller, “Creation of effective magnetic fields in optical lattices: the Hofstadter butterfly for cold neutral atoms,” *New J. Phys.* **5**, 56 (2003).
- [44] X. G. Wen and Q. Niu, “Ground-state degeneracy of the fractional quantum hall states in the presence of a random potential

- and on high-genus riemann surfaces,” *Phys. Rev. B* **41**, 9377–9396 (1990).
- [45] Yasuhiro Hatsugai, “Characterization of topological insulators: Chern numbers for ground state multiplet,” *Journal of the Physical Society of Japan* **74**, 1374–1377 (2005), <https://doi.org/10.1143/JPSJ.74.1374>.
- [46] K. J. Maschhoff and D. C. Sorensen, “P\_arpac: An efficient portable large scale eigenvalue package for distributed memory parallel architectures,” in *Applied Parallel Computing Industrial Computation and Optimization*, edited by Jerzy Waśniewski, Jack Dongarra, Kaj Madsen, and Dorte Olsen (Springer Berlin Heidelberg, Berlin, Heidelberg, 1996) pp. 478–486.